Cryptotanshinone Inhibits Constitutive Signal Transducer and Activator of Transcription 3 Function through Blocking the Dimerization in DU145 Prostate Cancer Cells

Dae-Seop Shin,[1,2] Hye-Nan Kim,[1] Ki Deok Shin,[1] Young Ju Yoon,[1,2] Seung-Jun Kim,[1] Dong Cho Han,[1] and Byoung-Mog Kwon[1,2]

[1]Laboratory of Chemical Biology and Chemical Genomics Korea Research Institute of Bioscience and Biotechnology, and
[2]Korea University of Science and Technology, 52 Uendong Yoosunggu, Daejeon, Korea

Abstract

Because signal transducer and activator of transcription 3 (STAT3) is constitutively activated in most human solid tumors and is involved in the proliferation, angiogenesis, immune evasion, and antiapoptosis of cancer cells, researchers have focused on STAT3 as a target for cancer therapy. We screened for natural compounds that inhibit the activity of STAT3 using a dual-luciferase assay. Cryptotanshinone was identified as a potent STAT3 inhibitor. Cryptotanshinone rapidly inhibited STAT3 Tyr705 phosphorylation in DU145 prostate cancer cells and the growth of the cells through 96 hours of the treatment. Inhibition of STAT3 Tyr705 phosphorylation in DU145 cells decreased the expression of STAT3 downstream target proteins such as cyclin D1, survivin, and Bcl-xL. To investigate the cryptotanshinone inhibitory mechanism in DU145 cells, we analyzed proteins upstream of STAT3. Although phosphorylation of Janus-activated kinase (JAK) 2 was inhibited by 7 μmol/L cryptotanshinone at 24 hours, inhibition of STAT3 Tyr705 phosphorylation occurred within 30 minutes and the activity of the other proteins was not affected. These results suggest that inhibition of STAT3 phosphorylation is caused by a JAK2-independent mechanism, with suppression of JAK2 phosphorylation as a secondary effect of cryptotanshinone treatment. Continuing experiments revealed the possibility that cryptotanshinone might directly bind to STAT3 molecules. Cryptotanshinone was colocalized with STAT3 molecules in the cytoplasm and inhibited the formation of STAT3 dimers. Computational modeling showed that cryptotanshinone could bind to the SH2 domain of STAT3. These results suggest that cryptotanshinone is a potent anticancer agent targeting the activation STAT3 protein. It is the first report that cryptotanshinone has antitumor activity through the inhibition of STAT3. [Cancer Res 2009;69(1):193–202]

Introduction

Signal transducers and activators of transcription (STAT) proteins are a family of seven proteins (STATs 1, 2, 3, 4, 5a, 5b, and 6) that transduce extracellular signals and regulate transcription of target genes. Among the STATs, STAT3 is the most intimately linked to tumorigenesis (1). STAT3 is constitutively activated and overexpressed in various tumor types such as breast carcinoma, prostate cancer, melanoma, multiple myeloma, and leukemia.

STAT3 activation involves phosphorylation on a critical tyrosine residue, Tyr705, by Janus-activated kinases (JAK; refs. 2, 3) and Rac1 (4). It was previously reported that STAT3 is phosphorylated on Tyr705 through the interleukin (IL)-6/gp130/JAK pathway in breast cancer cells (5). Another STAT3 Tyr705 phosphorylation mechanism involves Src family kinases. There are several reports that Src tyrosine kinase activates STAT3 and Src and STAT3 are coordinately altered in many human tumors (6–8). Phosphorylation of STAT3 on Tyr705 results in homodimerization or heterodimerization of STAT3, enabling nuclear localization and DNA binding (3). Subsequently, STAT3 is phosphorylated on Ser727, which enhances its transcriptional regulatory activities (9). In human breast cancer cell lines, phosphorylation of STAT3 Ser727 is associated with the expression or constitutive activation of epidermal growth factor receptor (10). STAT3 Ser727 phosphorylation is mediated by serine threonine kinases, including mitogen-activated protein kinase (MAPK), c-Jun-NH_2-kinase (JNK), and p38 (11–13). Fully activated, dimerized STAT3 molecules bind to specific DNA response elements and regulate specific target genes. These target genes include antiapoptotic proteins (Bcl-xL, Bcl-2; ref. 14), proliferation regulatory proteins (Cyclin D1, survivin; refs. 15, 16), and angiogenesis proteins [vascular endothelial growth factor (VEGF); ref. 17]. STAT3 is also responsible for the antiimmune response of tumor cells through the blockade of proinflammatory factor expression (18).

Because of the critical role of STAT3 in tumor cell survival and its expression in various tumor cells, and the fact that natural products are still a major source for new drug development (19), we have screened 3,025 plant extracts, including 342 herbal medicines and identified modulators of STAT3 activity. We found that cryptotanshinone from *Salvia miltiorrhiza* Bunge (Danshen) inhibited the phosphorylation of STAT3. Dried roots of *Salvia miltiorrhiza* Bunge (Danshen) have commonly been used in traditional oriental medicine for the treatment of circulatory disorders, liver disease (20, 21), coronary heart disease, hepatitis, and chronic renal failure (22). Two major tanshinones, cryptotanshinone and tanshinone IIA, are well-known active components in this herbal plant. Tanshinone IIA had been reported to have an anti-inflammatory effect through the inhibition of proinflammatory mediators such as NO, tumor necrosis factor α, IL-1β, and IL-6 in RAW 264.7 cells (23). It was also reported that tanshinone IIA inhibited leukocyte chemotactic migration (24) and induced apoptosis in human hepatocellular carcinoma cells (25), human promyelocytic leukemic cells (26), and human erythroleukemic

Note: Supplementary data for this article are available at Cancer Research Online (http://cancerres.aacrjournals.org/).

Requests for reprints: Dong Cho Han, Phone: 82-42-860-4568; E-mail: dchan@kribb.re.kr and Byoung-Mog Kwon, KRIBB/UST, 52 Uendong Yoosung, Daejeon, 305-600, South Korea. Phone: 82-42-860-4557; Fax: 82-861-2675; E-mail: kwonbm@kribb.re.kr.

doi:10.1158/0008-5472.CAN-08-2575

cells (27, 28). Cryptotanshinone was previously observed to possess the most powerful antibacterial activity among the tanshinones that have been tested. It counteracts inflammation through the inhibition of cyclooxygenase II activity and endothelin-1 expression (29). However, there have been no reports on the possible antitumor effect of cryptotanshinone.

In this study, we investigated the mechanism of cryptotanshinone inhibition of STAT3 in tumor cells. Our results provide that cryptotanshinone selectively inhibits STAT3-activated cell lines through blocking the dimerization of STAT3.

Materials and Methods

Reagents. RPMI 1640, DMEM, McCoy's 5A, fetal bovine serum (FBS), and antibiotic-antimycotic solution were purchased from Life Technologies/Bethesda Research Laboratories. Antibodies against STAT3, p-STAT3^{Tyr705}, p-STAT3^{Ser727}, p-STAT1, p-STAT5, p-JAK1, p-JAK2, p-JAK3, p-Tyk2, p-Src p-p38, p-Akt, p-Erk1/2, p-PI3K, p-SAPK/JNK, and gp130 were purchased from Cell Signaling Technology. Antibodies against cyclin A, cyclin D1, Bcl-xL, VEGF, and β-actin were purchased from Santa Cruz Biotechnology, Inc. Goat-anti-rabbit and anti-mouse horseradish peroxidase (HRP) conjugates was purchased from Jackson ImmunoResearch Laboratories, Inc. DMSO and chemicals used in buffer solutions were purchased from Sigma-Aldrich Chemical Co. Cryptotanshinone was isolated from dried roots of *Salvia miltiorrhiza* Bunge (Danshen).

Cell culture. Cancer cell lines were obtained from American Type Culture Collection. A human stomach cell line (KATO III), human prostate cancer cell lines (DU145, PC3, and LNCaP), and human breast cancer cell lines (MDA-MB-231, MDA-MB-468, MDA-MB-453, MCF-7, and MCF-10A) were maintained in RPMI 1640. HeLa (human cervical adenocarcinoma cell line) cells were maintained in DMEM. HCT-116 (human colon cancer cell line) was maintained in McCoy's 5A. All culture medium was supplemented with 10% heat-inactivated FBS. Cell cultures were maintained at 37°C under a humidified atmosphere of 5% CO_2 in an incubator.

Cell proliferation assay. Proliferation assays were performed as described previously (30). Briefly, cells were seeded at a density of 5,000 cells per well in 96-well plates in RPMI 1640 containing 10% FBS. Cells were replenished with fresh complete medium containing either test compounds or 0.1% DMSO. After incubation for 24 or 48 h, the cell proliferation reagent WST-1 (Dojindo laboratories) was added to each well. WST-1 formazan was quantitatively measured at 450 nm using an ELISA reader (Bio-Rad Laboratories, Inc.).

Transient transfection and dual-luciferase assay. HCT-116 cells were seeded at a density of 10×10^5 cells in 100 mm^2 culture plates. On the following day, cells were transfected with 27 μg of 21pSTAT3-TA-Luc and 9 μg of pRL-TK, a *Renilla* luciferase control reporter plasmid (Promega) using TransFectin (Bio-Rad Laboratories). After 5 h of transfection, cells were trypsinized and seeded onto sterile, black-bottom 96-well plates at a density of 1×10^4 cells per well, and then incubated with complete medium for 24 h. Cells were treated with either test compounds or 0.1% DMSO for 24 h. After treatment, cells were harvested in 20 μL of passive lysis buffer and luciferase activity was evaluated by the Dual Luciferase Reporter Assay kit (Promega) on Wallac Victor2 (Perkin-Elmer, Inc.). Experiments were performed in triplicate and repeated three times. Relative luciferase activity was calculated as according to the formula: relative luciferase activity (%) = [(normalized luciferase activity of sample treated with a test compound)/(normalized luciferase activity of sample treated with 0.1% DMSO)] × 100.

Western blotting. Cell lysates were prepared by cell incubation in radioimmunoprecipitation assay buffer [RIPA; 50 mmol/L Tris (pH 7.4), 150 mmol/L NaCl, 5 mmol/L EDTA, 1% Triton X-100, 1% Sodium deoxycholic acid, 0.1% SDS, 2 mmol/L phenylmethylsulfonyl fluoride (PMSF), 30 mmol/L Na_2HPO_4, 50 mmol/L NaF, and 1 mmol/L Na_3VO_4] containing protease inhibitor cocktail (Roche Applied Science). Proteins (40 μg) were resolved on 7.5 or 10% SDS-PAGE and transferred to polyvinylidene difluoride (PVDF) membranes (Millipore Co.). Membranes were blocked with 5% nonfat dried milk in TBS-T [50 mmol/L Tris-HCl (pH 7.6), 150 mmol/L NaCl, and 0.1% Tween 20] and probed with primary antibodies for 3 h. Blots were washed with TBS-T and exposed to HRP-conjugated goat-anti-rabbit or goat-anti-mouse IgG for 1 h, and examined using chemiluminescence POD reagents (Roche Applied Science).

Native gel PAGE. Cell extracts containing native proteins were prepared using ice-cold isotonic buffer [20 mmol/L Tris (pH 7.0), 150 mmol/L NaCl, 6 mmol/L $MgCl_2$, 0.8 mmol/L PMSF, and 20% glycerol] as described previously (31). Lysates were homogenized using a 27-gauge syringe and then cleared by centrifugation at 13,000 rpm for 30 min at 4°C. Native PAGE analysis was carried out by loading 10 μg samples onto 6% SDS-free, PAGE gels. Proteins were transferred to PVDF membranes (Millipore) and immunoblotted with specific antibody as described for Western blotting.

Electrophoretic mobility shift assay. Nuclear protein extracts were prepared from DU145 prostate cancer cells as described previously (6). Briefly, cells were suspended in hypertonic buffer [20 mmol/L HEPES (pH 7.9), 420 mmol/L NaCl, 1 mmol/L EDTA, 1 mmol/L EGTA, 20% glycerol, 20 mmol/L NaF, 1 mmol/L Na_3VO_4, 1 mmol/L $Na_4P_2O_7$, 1 mmol/L DTT, 0.5 mmol/L phenylmethylsulfonyl fluoride, 0.1 μmol/L aprotinin, 1 μmol/L leupeptin, and 1 μmol/L antipain] and homogenized using a 27-guage syringe. Nuclear extracts were collected by centrifugation at 13,000 rpm for 30 min at 4°C. Protein concentrations were determined using a Protein Assay kit (Bio-Rad Laboratories) according to the manufacturer's protocol. Nuclear protein extracts (10 μg each) were incubated with a biotin-labeled, double-stranded STAT3 consensus-binding motif: high affinity sis-inducible element (hSIE; m67 variant) consensus sequence (sense strand; 5′-AGCTTCATTTCCCGTAAATCCCTA-3′) derived from the c-*fos* gene promoter. Binding reactions and electrophoresis were carried out using the LightShift Chemiluminescent electrophoretic mobility shift assay (EMSA) kit (Pierce Biotechnology, Inc.) according to the manufacturer's protocol. Protein-DNA complexes were resolved on 6% nondenaturing polyacrylamide gels, transferred to nylon membranes (Whatman), and cross-linked for 15 min under a hand-held UV lamp equipped with a 254-nm bulb. Cross-linked, biotin-labeled DNA was detected using the Chemiluminescent Nucleic Acid Detection Module (Pierce Biotechnology, Inc.).

Fluorescence-activated cell sorting analyses. Cells were trypsinized at specific times after compound treatment and collected by centrifugation at 300 × *g* for 5 min at room temperature. The supernatant was discarded and the precipitated cells were washed twice by repeating suspension and precipitation in PBS buffer. Precipitated cells were carefully suspended in 500 μL PBS buffer and fixed with 4 mL of ice-cold 70% ethanol overnight. Fixed cells were washed twice with PBS. The collected cells were resuspended in PBS (5×10^5 cells/500 μL) and treated with 100 μg/mL of RNase A at 37°C for 30 min. Propidium iodide (PI; Sigma) was then added at a final concentration of 50 μg/mL for DNA staining, and 20,000 fixed cells were analyzed on a FACScalibur (Becton Dickinson). Cell cycle distribution was analyzed using the Modifit program (Becton Dickinson).

Confocal laser microscopy. Coverslips for cell culture were immersed in 70% ethanol overnight and rinsed with PBS buffer [137 mmol/L NaCl, 2.7 mmol/L KCl, 4.3 mmol/L Na_2HPO_4, 1.4 mmol/L KH_2PO_4 (pH 7.4)]. Coverslips were laid in 6-well plates and cells were seeded at a density of 2.5×10^5 cells per well. After 24 h of treatment, cells were rinsed with PBS and fixed for 10 min at room temperature in 4% paraformaldehyde fixative, followed by permeabilization with 0.1% Triton X-100. Cells were blocked with 1.0% bovine serum albumin (BSA) in PBS for 1 h and incubated for 3 h at room temperature with p-STAT3^{Tyr705} or STAT3 antibodies diluted in PBS containing 1.0% BSA. After washing thrice in PBS buffer, the cells were incubated with FITC-conjugated goat-anti-mouse IgG (Santa Cruz Biotechnology, Inc.). Finally, the cells were washed thrice in PBS and treated with 2 μg/mL of PI in PBS for 5 min to stain chromosomes. Coverslips were washed in PBS and mounted on glass slides. Cells were observed using a Zeiss LSM 510 META confocal microscope (Carl Zeiss, Inc.).

STAT3 knockdown using STAT3 siRNA. The human STAT3 siRNA duplex and negative control siRNA were purchased from Bioneer, Inc. The sequences of each siRNA were as follows: negative control (sense, 5′-CCUACGCCACCAAUUUCGUdTdT-3′; antisense, 5′-ACGAAAUUGGUGGCGUAGGdTdT-3′), STAT3 siRNA-1 (sense, 5′-UGUUCUCUGAGACCCAUGAdTdT-3′; antisense, 5′-UCAUGGGUCUCAGAGAACAdTdT-3′), and

STAT3 siRNA-2 (sense, 5′-CUAUCUAAGCCCUAGGUUUdTdT-3′; antisense, 5′-AAACCUAGGGCUUAGAUAGdTdT-3′). Cells were plated at a density of 8×10^4 cells per well on 6-well plates and transfected with 100 nmol/L of STAT3-specific and control siRNA duplexes after incubation for 20 min with Oligofectamine RNAi Max (Invitrogen) in OPTI-MEM (Invitrogen). Five hours after transfection, siRNA and Oligofectamine mixtures were discarded and substituted with RPMI 1640 containing 10% serum.

Results

Cryptotanshinone inhibits STAT3-dependent luciferase activity in HCT-116 colon cancer cells. To identify a novel and specific inhibitor of STAT3, natural compounds were screened using a dual-luciferase assay system reflecting STAT3 activity. HCT-116 cells were transiently transfected with reporter plasmid having the STAT3-binding element for regulating luciferase assay. Cryptotanshinone, isolated from the roots of *Salvia miltiorrhiza* Bunge (Danshen), was identified as an inhibitor of STAT3. The structures of cryptotanshinone and tanshinone IIA, a known abietane derivative, are shown in Fig. 1*A*. HCT-116 colon cancer cells were transiently transfected with reporter plasmids and treated with cryptotanshinone or tanshinone IIA at a concentration range of 0.2 to 50 μmol/L for 24 hours to confirm a dose-dependent inhibition effect. Cryptotanshinone inhibited STAT3 activity in a dose-dependent manner, with an IC_{50} value of 4.6 μmol/L (Fig. 1*B*). However, tanshinone IIA did not inhibit STAT3 activity in STAT3-dependent dual-luciferase assays. Inhibition of STAT3 activity by cryptotanshinone was also obtained in several cancer cell lines having activated STAT3 such as MDA-MB-231, HeLa, and DU145 cell lines (Fig. 1*C*). These data strongly suggest that cryptotanshinone specifically inhibits STAT3 activity regardless of cell lines.

Cryptotanshinone inhibits the growth of DU145 cells harboring constitutively activated STAT3. To determine whether the suppression of STAT3 activity could induce growth inhibition in cancer cell lines, the expression level and activation status (STAT3 phosphorylated on Tyr705 and Ser727) of STAT3 was evaluated in various human cancer cell lines. Among these human cancer cell lines, the DU145 prostate cancer cell line, MDA-MB-468 breast carcinoma cell line, MDA-MB-231 breast carcinoma cell line, and HeLa cervix adenocarcinoma cell line displayed high levels of activated STAT3 as evidenced by STAT3 Tyr705 and Ser727 phosphorylation (Fig. 2*A*). It was previously reported that STAT3 knockdown induced the growth inhibition in breast (32) and prostate (33) cancer cells. Moreover, direct inhibition of constitutively activated STAT3 causes apoptosis in human prostate carcinoma cell lines (34–36). We next tested whether knockdown of STAT3 using siRNA induced growth inhibition in cancer cell lines. STAT3 was silenced by two different STAT3 siRNAs (STAT3 siRNA-1 and STAT3 siRNA-2) in various cancer cell lines (Supplementary Fig. S1). STAT3 siRNA-2 was introduced into human cancer cell lines and cell numbers were counted at a specific times as indicated. The proliferation of DU145 prostate cancer cells transfected with STAT3 siRNA-2 was dramatically suppressed after 48 hours. However, STAT3 knockdown in other cell lines showed only minimal inhibitory effects (Fig. 2*B*). It seemed that the growth of DU145 cells was most sensitive to the silencing of STAT3.

We examined whether the growth inhibition by cryptotanshinone was caused by inhibition of STAT3 activity in breast and prostate cancer cell lines. Cryptotanshinone showed significant growth inhibitory effect on the DU145 prostate cancer cell line with a GI_{50} value of 7 μmol/L. However, it did not inhibit the growth of PC3 and LNCaP cells at that concentration (Fig. 2*C*). Cryptotanshinone also had only a minimal growth inhibitory effect on three breast carcinoma cell lines. Although STAT3 showed high activity in MDA-MB-468 breast cancer cells, cryptotanshinone only inhibited growth by ~32%, even at a concentration of 50 μmol/L.

To test long-term effects of cryptotanshinone on cancer cell growth, 3 prostate cancer cell lines were treated with cryptotanshinone at a concentration of 7 μmol/L for up to 96 hours. When the cells was treated with cryptotanshinone, DU145 cell proliferation but not PC3 and LNCaP proliferation was significantly inhibited as shown in Fig. 2*D*. These data show that cryptotanshinone

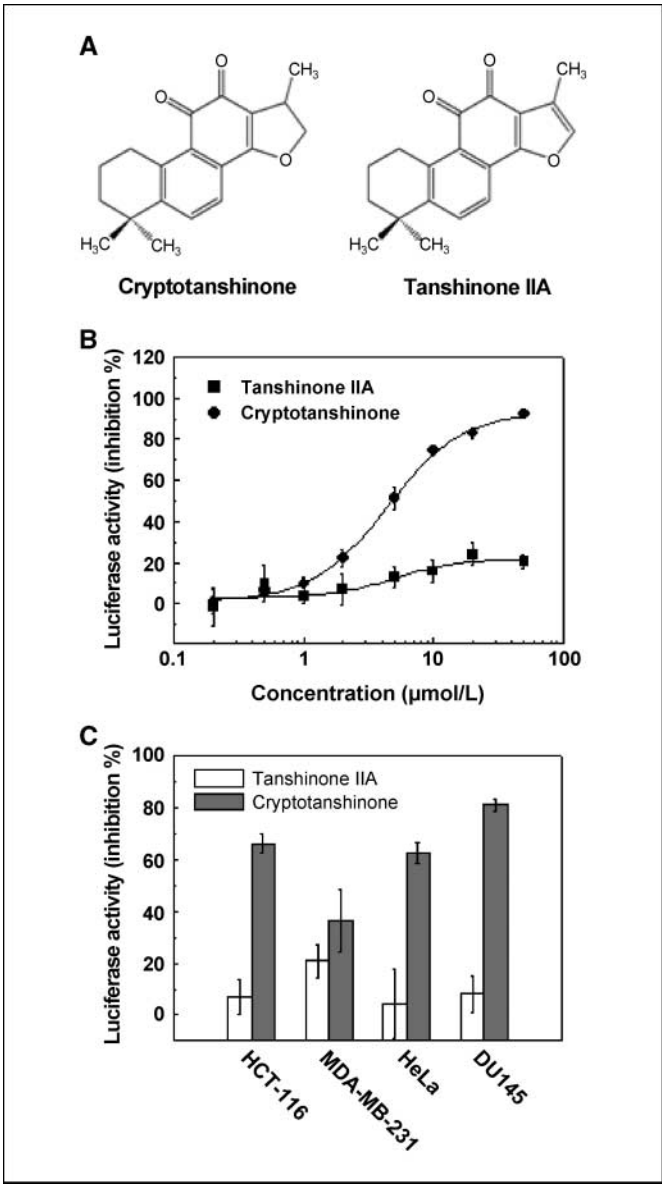

Figure 1. Cryptotanshinone inhibits STAT3-dependent luciferase activity. *A,* structure of cryptotanshinone and tanshinone IIA. *B,* HCT-116 cells were analyzed using a dual-luciferase assay. Luciferase assay was carried out as described in Materials and Methods. *C,* cryptotanshinone inhibits STAT3 activity in human cancer cell lines. Dual-luciferase assays were carried in MDA-MB-231, HeLa, DU 145, and HCT-116 after 24-h treatment with tanshinone IIA (7 μmol/L) and cryptotanshinone (7 μmol/L).

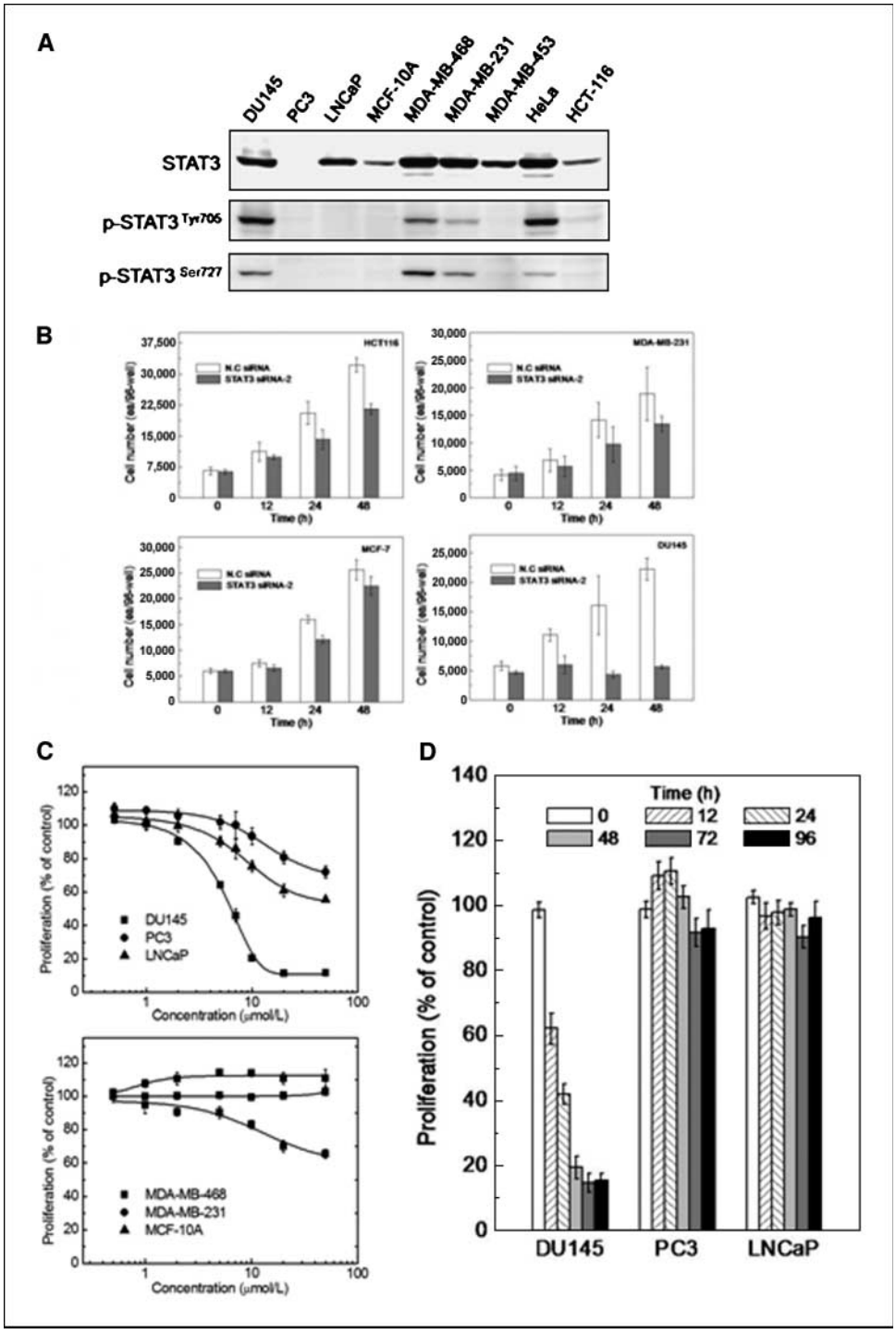

Figure 2. Cryptotanshinone sensitively inhibits prostate cancer cells harboring constitutively activated STAT3. *A,* levels of STAT3, p-STAT3^{Tyr705}, and p-STAT3^{Ser727} in various human cancer cell lines were detected by immunoblotting using specific antibody. *B,* human cancer cell lines were transfected with negative control siRNA and STAT3 siRNA-2, and cell number was counted with heamatocytometer at each time. HCT-116, MDA-MB-231, MCF-7, and DU145 cells were inhibited by STAT3 silencing. *C,* proliferation of prostate (*top*) and breast (*bottom*) cancer cell lines were measured by WST-1 assay kit at 24 h after the treatment. *D,* cells were seeded at a density of 5,000 cells per well in a 96-well microtiter plate. After 24 h, cells were treated with 0.1% DMSO or 7 μmol/L cryptotanshinone. WST-1 assay was carried out after incubation for different time.

selectively inhibits growth of the DU145 prostate cancer cell line that expresses constitutively active STAT3. DU145 cells were used for further studies to characterize the mode of action of cryptotanshinone.

Cryptotanshinone selectively suppresses STAT3 Tyr705 phosphorylation but not through inhibition of upstream tyrosine kinases. To clarify the mechanism of cryptotanshinone inhibition of STAT3 phosphorylation, the dose- and time-dependent effects of cryptotanshinone were evaluated by Western blot analyses of STAT family proteins. DU145 cells, treated with cryptotanshinone for 24 hours, led to a dramatic decrease in STAT3 Tyr705 phosphorylation, whereas phosphorylation of STAT3 Ser727 was only mildly decreased at the same concentration (Fig. 3*A*). The total amount of STAT3 protein remained unchanged during this time frame.

To investigate the selectivity and mechanism of STAT3 Tyr705 inhibition by cryptotanshinone, DU145 cells were treated with 7 μmol/L cryptotanshinone. Cell lysates were prepared for immunoblotting at different time points. The suppression of STAT3 Tyr705 phosphorylation occurred within 30 min (Fig. 3*B*). However,

the phosphorylation level of other STAT family proteins was not affected by cryptotanshinone until 4 hours after the treatment.

Because STAT3 Tyr705 is phosphorylated by soluble tyrosine kinases, various upstream kinases of STAT3 were analyzed in cell lysates after dose- and time-dependent treatment of cryptotanshinone. JAK family proteins and c-Src had been reported to activate STAT3 via Tyr705 phosphorylation (37). EGFR has been reported to be constitutively active in androgen-independent human prostate cancer cells such as the DU145 cell line (38). It was recently reported that EGFR is a receptor tyrosine kinase that induces the phosphorylation of STAT3 Ser727 through MAPK phosphorylation in DU145 cells (34). To investigate the mechanisms of inhibition for STAT3 Tyr705 phosphorylation, the activation level of upstream kinases, including phosphorylated JAK family proteins, c-Src, and EGFR were analyzed by Western blot. JAK2 phosphorylation was inhibited ~50% by 5 μmol/L cryptotanshinone, whereas the activating phosphorylation levels of the other proteins were not changed by cryptotanshinone (Fig. 3*C*). The level of phosphorylated JAK2 was suppressed after 4 hours of cryptotanshinone treatment in DU145 cells (Fig. 3*D*). However, inhibition of JAK2 phosphorylation was a later event than the inhibition of the STAT3 Tyr705 phosphorylation as shown in Fig. 3*B* and *D*. Also, phosphorylation of gp130 was not affected by cryptotanshinone (Supplementary Fig. S2). These results imply that the inhibition of STAT3 Tyr705 phosphorylation occurred through a mechanism that was independent of the IL-6/JAK/STAT3 pathway. These data suggested the possibility that cryptotanshinone might directly and specifically inhibit the phosphorylation of STAT3 Tyr705.

To determine the effect of cryptotanshinone on other survival pathways, the activating phosphorylation levels of cytosolic kinases such as extracellular signal-regulated kinase 1/2, p38, Akt, PI3K, and SAPK/JNK was analyzed by Western blot (Supplementary Fig. S3). Cryptotanshinone had no effect on the phosphorylation of these kinases.

Cryptotanshinone down-regulates the expression of cyclin D1, Bcl-xL, and survivin, and causes the accumulation of cells in G_0-G_1. Active STAT3 regulates the expression of target proteins involved in cell survival, proliferation, and angiogenesis through binding to specific sequences in the promoter region of target genes (39, 40). We investigated whether the expression of cyclin A and cyclin D1 (mediating cell cycle progression), Bcl-xL, survivin, p53 (in relation to its apoptotic properties), and VEGF was affected by cryptotanshinone treatment. Cryptotanshinone treatment suppressed the expression of cyclin D1, Bcl-xL, and survivin in a dose-dependent manner at 24 hours (Fig. 4*A*). To examine the effects of down-regulation of these proteins on cell cycle progress, fluorescence-activated cell sorting analysis was performed on DU145 cells treated with different concentrations of cryptotanshinone for 24 hours. Cell cycle distribution was analyzed by FACScaliber

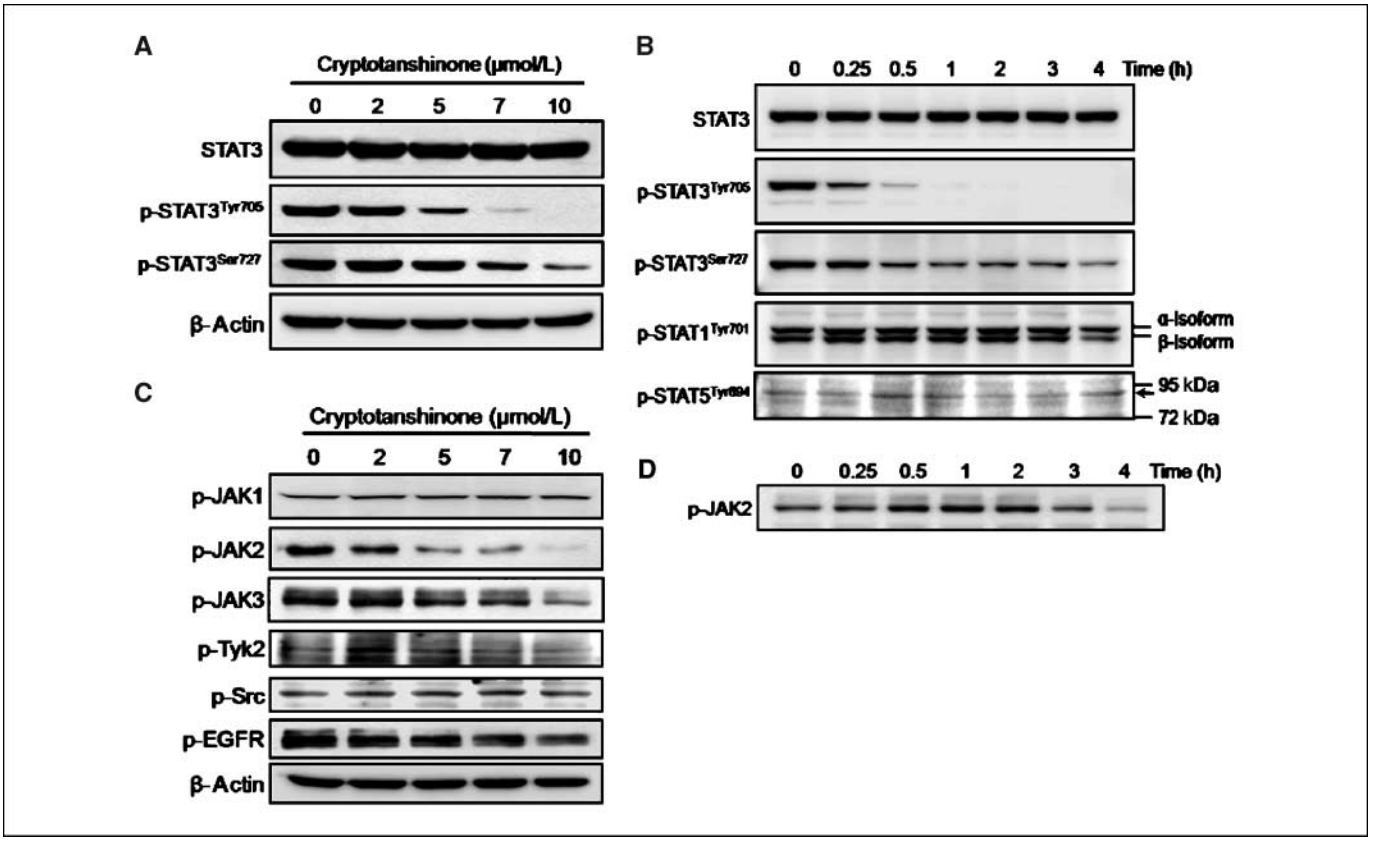

Figure 3. Cryptotanshinone inhibits phosphorylation of STAT3 Tyr705 independent of JAK2 activity. DU145 cells were dose- and time-dependently treated with cryptotanshinone. Cell lysates were prepared with RIPA lysis buffer. Proteins were analyzed by immunoblotting with specific antibodies. *A,* cryptotanshinone inhibited the phosphorylation of STAT3 Tyr705 in a dose-dependent manner, whereas phosphorylation of Ser727 was mildly inhibited. *B,* cryptotanshinone suppressed phosphorylated STAT3 levels within 30 min. DU145 cells were treated with 7 μmol/L cryptotanshinone for the indicated times. *C,* cryptotanshinone decreased the phosphorylation of JAK2 protein at the same concentration that suppressed Tyr705 phosphorylation. *D,* phosphorylation of JAK2 was analyzed in a time-dependent manner after treatment of cryptotanshinone. Cryptotanshinone did not induce meaningful inhibition of JAK2 phosphorylation.

(Fig. 4*B*). Cryptotanshinone concentrations over 7 μmol/L caused DU145 cells to accumulate in the G_0-G_1 phase. This result could be attributed to down-regulation of cyclin D1 expression caused by decreased STAT3 transcriptional regulatory activity. It has been reported that cyclin D1, which is required for cell cycle progression from the G_1 phase to the S phase, is regulated by STAT3 (41). The sub-G_1 population of cells, interpreted as low DNA content apoptotic cells, was increased by 10 μmol/L cryptotanshinone. Cryptotanshinone at dose of 15 μmol/L induced the accumulation of 52% of cells in sub-G_1 or apoptotic cells. As shown in Fig. 4*A*, these results may be due to the suppression of Bcl-xL and survivin, which are responsible for anti-apoptosis signaling.

Cryptotanshinone binds to STAT3 monomer and inhibits the dimerization of STAT3. To visualize cryptotanshinone inhibition of STAT3 localization in intact cells, immunofluorescence assays were carried out in HeLa cells using confocal microscopy. Cells were seeded on coverslips and treated with cryptotanshinone or tanshinone IIA for 2 hours, and then cells were fixed, stained, and observed under the microscope. In normal conditions, STAT3 was mainly located in the nucleus (Fig. 5*A, a*). Owing to chemical property of cryptotanshinone or tanshinone IIA molecules, we could detect its localization inside of cells. No fluorescence signal was detected in the absence of the cryptotanshinone or tanshinone IIA (Fig. 5*A, b*). To detect the change in localization of STAT3, cells were treated with cryptotanshinone or tanshinone IIA for 2 hours. Tanshinone IIA, used as a negative control, did not show meaningful change in localization of STAT3 as well as the total amount of STAT3 (Fig. 5*A, e*). Also, tanshinone IIA was ubiquitously located in the cytoplasm and nucleus independent of the location of STAT3 (Fig. 5*A, f*). However, STAT3 molecules were mainly located in the cytoplasm after treatment with cryptotanshinone, implying that cryptotanshinone inhibits the translocation of STAT3 into the nucleus (Fig. 5*A, i*). Moreover, cryptotanshinone was mainly located in the cytoplasm along with the STAT3 molecule but not in the nucleus (Fig. 5*A, j*). Differences in distribution between tanshinone IIA and cryptotanshinone are clearly shown in red circles indicating the nucleus.

HeLa cells were stained for phosphorylated $STAT3^{Tyr705}$ to confirm that cryptotanshinone inhibits STAT3 Tyr705 phosphorylation. In the growing condition, phosphorylated $STAT3^{Tyr705}$ molecules were concentrated in the nucleus (Fig. 5*B, a*). Treating cells with tanshinone IIA did not diminish phosphorylated $STAT3^{Tyr705}$ in the nucleus (Fig. 5*B, e*). However, cryptotanshinone dramatically decreased STAT3 Tyr705 phosphorylation (Fig. 5*B, i*). Tanshinone IIA was detected in the cytoplasm as well as in the nucleus (Fig. 5*B, f*). However, cryptotanshinone was only located in the cytoplasm but not in the nucleus (Fig. 5*B, j*). These data implies that cryptotanshinone directly binds to STAT3 molecules in the cytoplasm and thus inhibit Tyr705 phosphorylation, preventing STAT3 molecules from being translocated into the nucleus.

Because STAT3 Tyr705 phosphorylation is related with STAT3 dimerization, we analyzed whether cryptotanshinone inhibited STAT3 dimerization by using native PAGE. As shown in Fig. 5*C*, Cryptotanshinone decreased the amounts of dimerized STAT3 in DU145 cells in a time-dependent manner. Six hours after cryptotanshinone treatment, dimerized STAT3 was significantly decreased.

Dimerized STAT3 is an active form that has the ability to bind to *cis*-acting sequences in the promoters of target genes (42). Therefore, we further confirmed that cryptotanshinone decrease STAT3 dimers using an EMSA assay. For this, we treated DU145 cells with cryptotanshinone for different times and lysates were prepared. As shown in Fig. 5*D*, DNA binding activity of STAT3 was decreased after 3-hour treatment and almost completely lost after 6-hour treatment. These data suggest that cryptotanshinone binds to STAT3 monomers, blocking dimerization, and inhibiting STAT3 transcriptional regulatory activity.

Cryptotanshinone binds to the SH2 domain of STAT3. STAT3 dimerization is known to occur through the interaction of the SH2

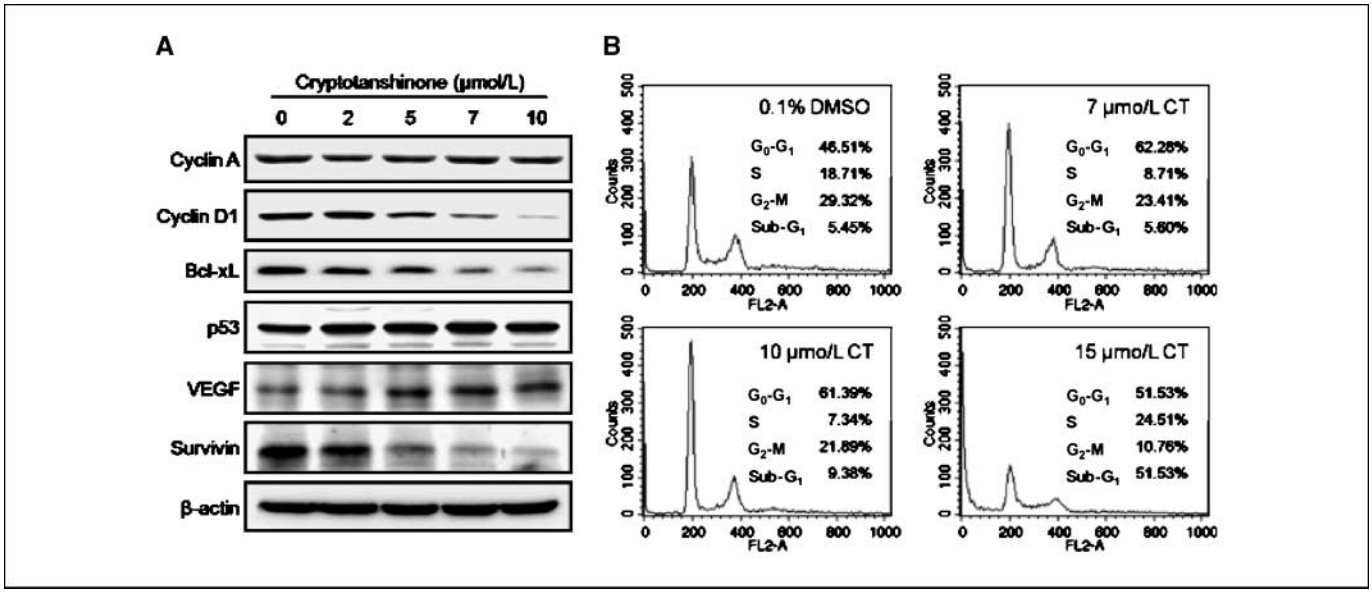

Figure 4. Cryptotanshinone inhibits STAT3-targeted proteins and induces accumulation of cells at the G_0-G_1 phase of the cell cycle or apoptosis in DU145 cells. *A,* DU145 cells were treated with cryptotanshinone in a dose-dependent manner. Downstream proteins regulated by STAT3 activity were subjected to immunoblotting with specific antibodies. *B,* cell cycle distribution was analyzed by FACSCalibur. Increased cryptotanshinone treatment induced a slowing of cell cycle progression in G_0-G_1 and apoptosis of DU145 cells.

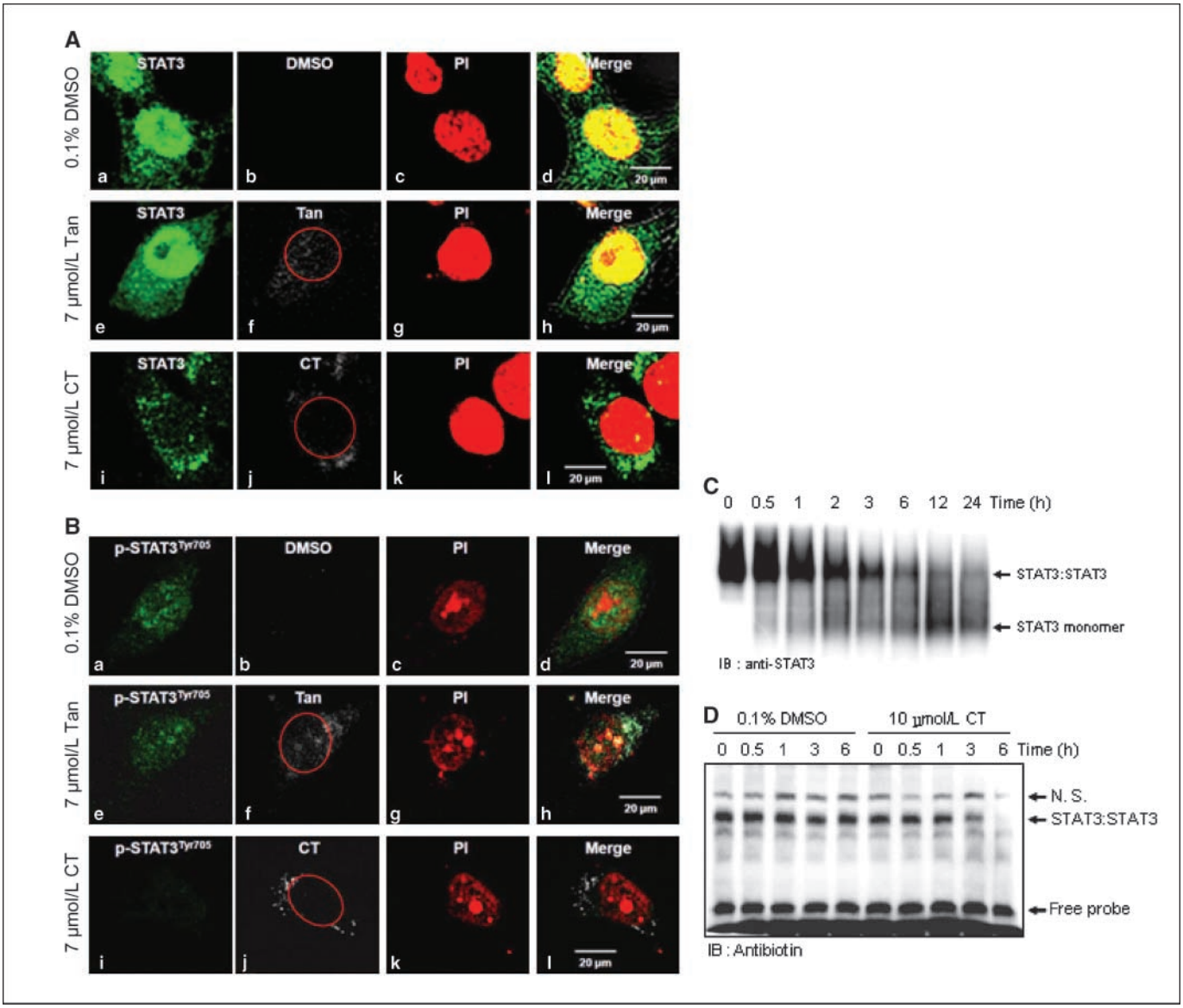

Figure 5. Cryptotanshinone binds to STAT3 molecules and decreases STAT3 dimerization. *A,* colocalization of cryptotanshinone with STAT3 in cytoplasm. HeLa cells were incubated in the absence and presence of 7 μmol/L cryptotanshinone or tanshinone IIA. After 2 h, cells were fixed with 4% paraformaldehyde and stained for STAT3, followed by a FITC-conjugated secondary antibody and propidium iodide. Cryptotanshinone and tanshinone IIA was visualized by the filter detecting 4′,6-diamidino-2-phenylindole fluorescence (excitation, 350 nm; emission, 470 nm). *a, e*, and *i,* localization of STAT3 (*green*). *b, f*, and *j,* localization of cryptotanshinone or tanshinone IIA (*white*). *c, g*, and *k,* staining for PI (*red*). *d, h*, and *l,* merging images STAT3, small-molecules, and PI. *B,* inhibition of p-STAT3^{Tyr705} by cryptotanshinone and localization of cryptotanshinone in the cytoplasm. Staining procedure was same in *A* except antibody for STAT3 was replaced by antibody for p-STAT3^{Tyr705}. *a, e*, and *i,* localization of p-STAT3^{Tyr705} (*green*). *b, f*, and *j,* localization of cryptotanshinone or tanshinone IIA (*white*). *c, g*, and *k,* staining for PI (*red*). *d, h*, and *l,* merging images p-STAT3^{Tyr705}, small-molecules, and PI. *C,* native protein extracts were prepared from DU145 cells at different times after treatment of cryptotanshinone. Ten micrograms of protein per sample was loaded onto a 5% native PAGE gel, and electrophoresis was performed in the absence of SDS. Proteins were transferred to a PVDF membrane and then immunoblotted (*IB*) with a STAT3 monoclonal antibody. Detailed descriptions of procedures are described in Materials and Methods. *D,* activity of STAT3 from DU145 cells treated with cryptotanshinone for different times was examined by EMSA assay using a hSIE probe.

domain on one STAT3 molecule with a loop segment (from Ala702 to Phe716) on the other STAT3 monomer (43, 44). The phosphorylated Tyr705 on one STAT3 molecule is a critical residue for binding to a cavity on the SH2 domain of the other STAT3 protein. Because of this reason, researchers have developed STAT3 inhibitors targeting the SH2 domain and evaluated their activity in cancer cells. In previous reports, structure-based virtual screening had been used to identify candidate compounds that can disrupt STAT3 dimerization (45, 46). The SH2 domain structure was used for virtual screening of small molecules.

To test whether cryptotanshinone can bind to the STAT3 SH2 domain, computational modeling was performed. The crystal structure of STAT3 at 2.25-Å resolution (43) was obtained from the Protein Data Bank (PDB ID code 1BG1) and used for this modeling. The results of this modeling approach indicated that cryptotanshinone could possibly bind to the SH2 domain of STAT3 (Fig. 6*A*). The mode of cryptotanshinone binding to STAT3 was predicted using the AutoDock 1.0 program (47) and the image of the predicted interaction was processed with the graphic program PyMOL. The refined model predicted that cryptotanshinone binds

at the specific site where the Tyr705 residue interacts within the SH2 domain (Fig. 6*B*). The model also predicted that cryptotanshinone forms a number of hydrogen bonds with nearby amino acid residues, including Arg609 and Ile634 (Fig. 6*C*).

Discussion

In this study, primary screening with a dual-luciferase assay was used for identification of STAT3 inhibitors. We selected cryptotanshinone as a small-molecule inhibitor of STAT3 transcriptional regulatory activity. It was previously reported that cryptotanshinone, together with tanshinone IIA, is one of major active components of the traditional medicinal ingredient *Salvia miltiorrhiza* Bunge (Danshen). Tanshinone IIA was excluded in this study because it did not show inhibitory activity in the luciferase assay (Fig. 1*B* and *C*). Therefore, we decided to characterize the mechanism of action of cryptotanshinone inhibition of STAT3 activity.

It was previously reported that knockdown of STAT3 induces apoptosis in human prostate cancer cell lines (33, 36). In this study, we confirmed that knockdown of STAT3 inhibits the proliferation of prostate cancer cells. As shown in Fig. 2*B*, knockdown of STAT3 protein by STAT3 siRNA caused cancer cell growth inhibition, although the efficiency of inhibition was different depending on the cell type. In particular, growth of DU145 prostate cancer cells was inhibited >60% by treatment with STAT3 siRNA. Therefore, DU145 cell was selected for the mechanism studies of STAT3 inhibitors.

Next, we tested cryptotanshinone growth inhibition effect in prostate and breast cancer cell lines harboring different levels of STAT3 activity. As shown in Fig. 3*C*, the inhibitory effect was dependent on the STAT3 activation status in three prostate cancer cell lines. DU145 cells showed the greatest sensitively to cryptotanshinone inhibition. In DU145 cells, cryptotanshinone strongly inhibited phosphorylation of STAT3 Tyr705 but had only a small effect on STAT3 Ser727 at 7 μmol/L (Fig. 3*A*). Interestingly, effects on tyrosine residue phosphorylation were only observed for STAT3 and not STAT1 or STAT5 within 30 min (Fig. 3*B*). These data suggest that cryptotanshinone specifically blocks the phosphorylation of STAT3 Tyr705.

To investigate the mechanism of cryptotanshinone-induced STAT3 inhibitory effects in DU145 cells, we analyzed the activation of upstream proteins such as JAK family proteins and Src. The IL-6/gp130/JAK signaling pathway is well-established as a signaling pathway that phosphorylates STAT3 Tyr705 in human fibrosarcoma cells (2), breast cancer cell (5), and myeloid cell (48). As shown in Fig. 3*C*, only phosphorylation of JAK2 was suppressed by treatment with 7 μmol/L cryptotanshinone. However, it was likely that the inhibition of STAT3 Tyr705 was not due to inhibition of JAK2 activity because the inhibition of JAK2 phosphorylation occurred 4 hours after the treatment, whereas STAT3 phosphorylation was inhibited within 30 minutes after the treatment (Fig. 3*D*). These results suggest that inhibition of STAT3 Tyr705 phosphorylation by cryptotanshinone is not due to proteins related to the JAK/STAT pathway. Also, activity of various cytosolic kinases responsible for cell proliferation, angiogenesis, and cell division were not affected after the cryptotanshinone treatment (Supplementary Fig. S3). These results strongly support the possibility that the growth inhibition of DU145 cells is due to STAT3 inactivation through an unknown pathway.

It was possible that the antitumor effects of cryptotanshinone might be mediated by suppressing the expression of STAT3-regulated target genes such as cyclin D1, survivin, and Bcl-xL.

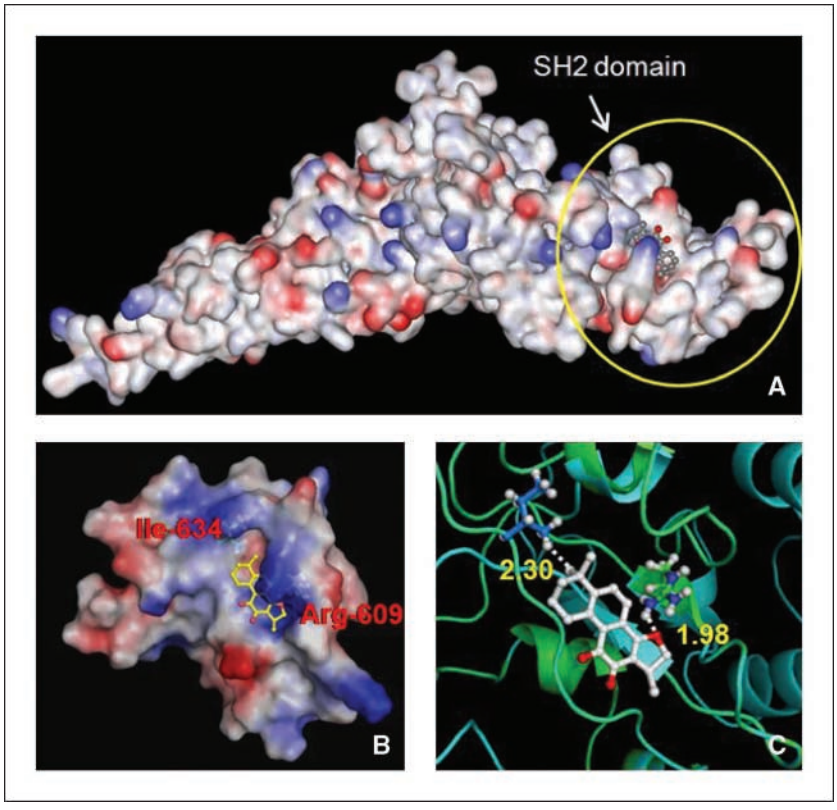

Figure 6. Schematic diagrams of cryptotanshinone docking with the STAT3 SH2 domain. *A,* predicted model of cryptotanshinone binding to the STAT3β SH2 as shown by computational modeling. Protein structure information was obtained from Protein Data Bank entry 1BG1. *B,* binding model of cryptotanshinone to the SH2 domain. The molecular surface of STAT3β SH2 domain is electrostatically colored with blue and red representing potentially positive and negative charged regions, respectively. *C,* predicted interaction between the amino acid residues of the SH2 domain and cryptotanshinone. *Red,* oxygen atoms of cryptotanshinone are shown in red. Hydrogen bonding is shown between Arg609 and cryptotanshinone. The hydrophobic ring of cryptotanshinone is located toward Ile634.

Down-regulation of these proteins inhibited cell cycle progression and led to inhibition of cell growth. STAT3 phosphorylation plays a critical role in the proliferation of tumor cells (39). The down-regulation of cyclin D1 expression by cryptotanshinone was correlated with accumulation of cells in the G_1 phase of the cell cycle. Also, the suppression of Bcl-xL expression by cryptotanshinone seemed to induce cell death (Fig. 4*B*). It has been reported that Bcl-xL can also block cell death induced by a variety of chemotherapeutic agents in parallel with an increase in chemoresistance (49). The down-regulation of the Bcl-xL and survivin is likely linked with the ability of cryptotanshinone to induce cell death in DU145 cells.

The localization experiments with confocal microscopy implied that cryptotanshinone might bind to STAT3 molecules directly. Weak cryptotanshinone fluorescence at 470 nm by excitation at 350 nm was used for localization of cryptotanshinone within the cells. When cells were treated with cryptotanshinone, most of STAT3 was localized in the cytoplasm such as cryptotanshinone. This colocalization of cryptotanshinone with STAT3 implied that cryptotanshinone bind directly to STAT3 (Fig. 5*A* and *B*). Using computational modeling, we found that cryptotanshinone may directly bind to the SH2 domain of STAT3. Computational modeling also showed the mode of interaction through which cryptotanshinone interacts with Arg609 and Ile634 residues in STAT3 (Fig. 6*B*). From these examinations, it seems that interaction at the SH2 pocket of STAT3 allows cryptotanshinone to inhibit the phosphorylation and dimerization of STAT3.

Other investigators have reported by computational modeling that STAT3 dimerization is achieved through an interaction between the phosphorylated Tyr705 residue of one STAT3 monomer and the SH2 domain of the other STAT3. Therefore, the SH2 domain had been regarded as a target site of for the development of STAT3 inhibitors and small-molecules that bind to the SH2 domain have been virtually screened (45, 46). We are proposing that destabilization of STAT3 dimers could be induced by the direct binding of cryptotanshinone to the SH2 domain of STAT3.

This is the first report of cryptotanshinone as a novel inhibitor of STAT3 signaling. Cryptotanshinone specifically suppressed STAT3 signaling and not other proteins in the STAT family. Moreover, cryptotanshinone did not down-regulate STAT3 protein expression, even at the highest concentrations tested. It has been reported that curcumin, an inhibitor of the STAT pathway, decreased STAT3 expression itself after 24 hours of treatment (50). However, in the present investigations, STAT3 expression did not decrease in DU145 cells after cryptotanshinone treatment. These results suggest that cryptotanshinone is a more specific STAT3 inhibitor than previously reported small molecules, without general cytotoxic effects.

Disclosure of Potential Conflicts of Interest

No potential conflicts of interest were disclosed.

Acknowledgments

Received 7/5/2008; revised 9/25/2008; accepted 10/15/2008.

Grant support: Plant Diversity Research Center of the 21st Century Frontier Research Program, the Korea Research Institute of Bioscience and Biotechnology Research Initiative Program, the National Chemical Genomics Research Program, and the Center for Biological Modulators of the 21st Century Frontier Research Program.

The costs of publication of this article were defrayed in part by the payment of page charges. This article must therefore be hereby marked *advertisement* in accordance with 18 U.S.C. Section 1734 solely to indicate this fact.

References

1. Aggarwal BB, Sethi G, Ahn KS, et al. Targeting signal-transducer-and-activator-of-transcription-3 for prevention and therapy of cancer: modern target but ancient solution. Ann N Y Acad Sci 2006;1091:151–69.
2. Guschin D, Rogers N, Briscoe J, et al. A major role for the protein tyrosine kinase JAK1 in the JAK/STAT signal transduction pathway in response to interleukin-6. EMBO J 1995;14:1421–9.
3. Darnell JE, Jr. STATs and gene regulation. Science 1997;277:1630–5.
4. Simon AR, Vikis HG, Stewart S, Fanburg BL, Cochran BH, Guan KL. Regulation of STAT3 by direct binding to the Rac1 GTPase. Science 2000;290:144–7.
5. Berishaj M, Gao SP, Ahmed S, et al. Stat3 is tyrosine-phosphorylated through the interleukin-6/glycoprotein 130/Janus kinase pathway in breast cancer. Breast Cancer Res 2007;9:R32.
6. Yu CL, Meyer DJ, Campbell GS, et al. Enhanced DNA-binding activity of a Stat3-related protein in cells transformed by the Src oncoprotein. Science 1995;269:81–3.
7. Zhang Y, Turkson J, Carter-Su C, et al. Activation of Stat3 in v-Src-transformed fibroblasts requires cooperation of Jak1 kinase activity. J Biol Chem 2000;275:24935–44.
8. Garcia R, Bowman TL, Niu G, et al. Constitutive activation of Stat3 by the Src and JAK tyrosine kinases participates in growth regulation of human breast carcinoma cells. Oncogene 2001;20:2499–513.
9. Wen Z, Darnell JE, Jr. Mapping of Stat3 serine phosphorylation to a single residue (727) and evidence that serine phosphorylation has no influence on DNA binding of Stat1 and Stat3. Nucleic Acids Res 1997;25:2062–7.
10. Sartor CI, Dziubinski ML, Yu CL, Jove R, Ethier SP. Role of epidermal growth factor receptor and STAT-3 activation in autonomous proliferation of SUM-102PT human breast cancer cells. Cancer Res 1997;57:978–87.
11. Chung J, Uchida E, Grammer TC, Blenis J. STAT3 serine phosphorylation by ERK-dependent and -independent pathways negatively modulates its tyrosine phosphorylation. Mol Cell Biol 1997;17:6508–16.
12. Sengupta TK, Talbot ES, Scherle PA, Ivashkiv LB. Rapid inhibition of interleukin-6 signaling and Stat3 activation mediated by mitogen-activated protein kinases. Proc Natl Acad Sci U S A 1998;95:11107–12.
13. Lim CP, Cao X. Serine phosphorylation and negative regulation of Stat3 by JNK. J Biol Chem 1999;274:31055–61.
14. Catlett-Falcone R, Dalton WS, Jove R. STAT proteins as novel targets for cancer therapy. Signal transducer an activator of transcription. Curr Opin Oncol 1999;11:490–6.
15. Sinibaldi D, Wharton W, Turkson J, Bowman T, Pledger WJ, Jove R. Induction of p21WAF1/CIP1 and cyclin D1 expression by the Src oncoprotein in mouse fibroblasts: role of activated STAT3 signaling. Oncogene 2000;19:5419–27.
16. Aoki Y, Feldman GM, Tosato G. Inhibition of STAT3 signaling induces apoptosis and decreases survivin expression in primary effusion lymphoma. Blood 2003;101:1535–42.
17. Niu G, Wright KL, Huang M, et al. Constitutive Stat3 activity up-regulates VEGF expression and tumor angiogenesis. Oncogene 2002;21:2000–8.
18. Wang T, Niu G, Kortylewski M, et al. Regulation of the innate and adaptive immune responses by Stat-3 signaling in tumor cells. Nat Med 2004;10:48–54.
19. Newman DJ. Natural products as leads to potential drugs: an old process or the new hope for drug discovery? J Med Chem 2008;51:2589–99.
20. Stickel F, Brinkhaus B, Krahmer N, Seitz HK, Hahn EG, Schuppan D. Antifibrotic properties of botanicals in chronic liver disease. Hepatogastroenterology 2002;49:1102–8.
21. Zhou L, Zuo Z, Chow MS. Danshen: an overview of its chemistry, pharmacology, pharmacokinetics, and clinical use. J Clin Pharmacol 2005;45:1345–59.
22. Lu Y, Foo LY. Polyphenolics of Salvia-a review. Phytochemistry 2002;59:117–40.
23. Jang SI, Jeong SI, Kim KJ, et al. Tanshinone IIA from Salvia miltiorrhiza inhibits inducible nitric oxide synthase expression and production of TNF-α, IL-1β and IL-6 in activated RAW 264.7 cells. Planta Med 2003;69:1057–9.
24. Zhou Z, Zheng J, Xu W. [Study on the effect of ofloxacin and tanshinone II A on human leukocyte chemotactic migration *in vitro*]. Zhongguo Yi Xue Ke Xue Yuan Xue Bao 1997;19:232–5.
25. Tang Z, Tang Y, Fu L. Growth inhibition and apoptosis induction in human hepatoma cells by tanshinone II A. J Huazhong Univ Sci Technolog Med Sci 2003;23:166–8, 72.
26. Yuan SL, Wei YQ, Wang XJ, Xiao F, Li SF, Zhang J. Growth inhibition and apoptosis induction of tanshinone II-A on human hepatocellular carcinoma cells. World J Gastroenterol 2004;10:2024–8.
27. Sung HJ, Choi SM, Yoon Y, An KS. Tanshinone IIA, an ingredient of Salvia miltiorrhiza BUNGE, induces apoptosis in human leukemia cell lines through the activation of caspase-3. Exp Mol Med 1999;31:174–8.
28. Yoon Y, Kim YO, Jeon WK, Park HJ, Sung HJ. Tanshinone IIA isolated from Salvia miltiorrhiza BUNGE induced apoptosis in HL60 human premyelocytic leukemia cell line. J Ethnopharmacol 1999;68:121–7.

29. Jin DZ, Yin LL, Ji XQ, Zhu XZ. Cryptotanshinone inhibits cyclooxygenase-2 enzyme activity but not its expression. Eur J Pharmacol 2006;549:166–72.

30. Han DC, Lee MY, Shin KD, et al. 2′-benzoyloxycinnamaldehyde induces apoptosis in human carcinoma via reactive oxygen species. J Biol Chem 2004; 279:6911–20.

31. Braunstein J, Brutsaert S, Olson R, Schindler C. STATs dimerize in the absence of phosphorylation. J Biol Chem 2003;278:34133–40.

32. Ling X, Arlinghaus RB. Knockdown of STAT3 expression by RNA interference inhibits the induction of breast tumors in immunocompetent mice. Cancer Res 2005;65:2532–6.

33. Gao LF, Xu DQ, Shao YT, Zhao D, Zhao XJ. [Knockdown of STAT3 expression using siRNA inhibits the growth of prostate cancer cell lines]. Zhonghua Nan Ke Xue 2005;11:29–33, 7.

34. Agarwal C, Tyagi A, Kaur M, Agarwal R. Silibinin inhibits constitutive activation of Stat3, and causes caspase activation and apoptotic death of human prostate carcinoma DU145 cells. Carcinogenesis 2007; 28:1463–70.

35. Barton BE, Karras JG, Murphy TF, Barton A, Huang HF. Signal transducer and activator of transcription 3 (STAT3) activation in prostate cancer: Direct STAT3 inhibition induces apoptosis in prostate cancer lines. Mol Cancer Ther 2004;3:11–20.

36. Mora LB, Buettner R, Seigne J, et al. Constitutive activation of Stat3 in human prostate tumors and cell lines: direct inhibition of Stat3 signaling induces apoptosis of prostate cancer cells. Cancer Res 2002;62: 6659–66.

37. Lo RK, Cheung H, Wong YH. Constitutively active Gα16 stimulates STAT3 via a c-Src/JAK- and ERK-dependent mechanism. J Biol Chem 2003;278:52154–65.

38. Shuch B, Mikhail M, Satagopan J, et al. Racial disparity of epidermal growth factor receptor expression in prostate cancer. J Clin Oncol 2004;22:4725–9.

39. Yu H, Jove R. The STATs of cancer-new molecular targets come of age. Nat Rev Cancer 2004;4:97–105.

40. Bromberg JF, Wrzeszczynska MH, Devgan G, et al. Stat3 as an oncogene. Cell 1999;98:295–303.

41. Matsushime H, Roussel MF, Ashmun RA, Sherr CJ. Colony-stimulating factor 1 regulates novel cyclins during the G1 phase of the cell cycle. Cell 1991;65: 701–13.

42. Qian L, Chen L, Shi M, et al. A novel *cis*-acting element in Her2 promoter regulated by Stat3 in mammary cancer cells. Biochem Biophys Res Commun 2006;345:660–8.

43. Becker S, Groner B, Muller CW. Three-dimensional structure of the Stat3β homodimer bound to DNA. Nature 1998;394:145–51.

44. Berman HM, Westbrook J, Feng Z, et al. The Protein Data Bank. Nucleic Acids Res 2000;28:235–42.

45. Song H, Wang R, Wang S, Lin J. A low-molecular-weight compound discovered through virtual database screening inhibits Stat3 function in breast cancer cells. Proc Natl Acad Sci U S A 2005;102:4700–5.

46. Siddiquee K, Zhang S, Guida WC, et al. Selective chemical probe inhibitor of Stat3, identified through structure-based virtual screening, induces antitumor activity. Proc Natl Acad Sci U S A 2007;104: 7391–6.

47. DeLano WL. The case for open-source software in drug discovery. Drug Discov Today 2005;10:213–7.

48. Minami M, Inoue M, Wei S, et al. STAT3 activation is a critical step in gp130-mediated terminal differentiation and growth arrest of a myeloid cell line. Proc Natl Acad Sci U S A 1996;93:3963–6.

49. Simonian PL, Grillot DA, Nunez G. Bcl-2 and Bcl-XL can differentially block chemotherapy-induced cell death. Blood 1997;90:1208–16.

50. Blasius R, Reuter S, Henry E, Dicato M, Diederich M. Curcumin regulates signal transducer and activator of transcription (STAT) expression in K562 cells. Biochem Pharmacol 2006;72:1547–54.